Spark plasma sintering of a commercial TiAl 48-2-2 powder: Densification and creep analysis

David Martins, Fanny Grumbach, Audrey Simoulin, Pierre Sallot, Katia
Mocellin, Michel Bellet, Claude Estournès

Open Archive TOULOUSE Archive Ouverte (OATAO)

Spark plasma sintering of a commercial TiAl 48-2-2 powder: Densification and creep analysis

David Martins[a,b], Fanny Grumbach[a], Audrey Simoulin[a], Pierre Sallot[c], Katia Mocellin[b],
Michel Bellet[b], Claude Estournès[a,*]

[a] *Université de Toulouse, CIRMAT CNRS UPS INPT, 118 route de Narbonne, 31062 Toulouse cedex 9, France*
[b] *Mines ParisTech, PSL - Research University, CEMEF - Centre for Material Forming, CNRS UMR 7635, CS 10207 rue Claude Daunesse, 06904 Sophia-Antipolis Cedex, France*
[c] *SAFRAN Tech, Rue des Jeunes Bois, 78114 Magny-les-Hameaux, France*

ABSTRACT

Commercial 48-2-2 TiAl powder was densified by spark plasma sintering. Fully dense materials with duplex and lamellar microstructures were obtained. An original protocol was developed to avoid carbide formation due to reactions between TiAl and graphite molds. TiAl materials with lamellar microstructures and high creep behavior were produced.

1. Introduction

The intermetallic TiAl is now an industrial reality for structural applications such as aero-engine parts [1], as it is one of the most important candidates for the replacement of nickel-based superalloys [2–4]. It exhibits relatively high yield strength at high temperatures, good creep resistance, and excellent resistance to oxidation/corrosion; and its low density (3.9–4.1 g/cc) makes it very attractive for use in low-pressure turbines and turbochargers in the automotive industry [5]. Its production can be diverse and varied, including using classical fusion processes (vacuum arc remelting (VAR)), hot working techniques [3,4], and casting [6]. Usually, pure elements are mixed and melted during VAR. Then, centrifugal or gravity casting, depending on the complexity of the parts to produce, is used. The main drawbacks of such techniques are the control of chemical and microstructure homogeneity within the parts, which may generate dispersions of their mechanical properties. Powder metallurgy seems to be a way to circumvent some of these problems.

Spark plasma sintering (SPS) is similar to hot pressing (HP), but it is recognized as a non-conventional densification process [7]. Commonly, with HP, a uniaxial external load is applied to the powder, which produces much faster densification than with free sintering. Unlike HP, in SPS, the heat source is provided by the Joule effect, which is produced by a pulsed current applied through the tools [8]. Depending on the electrical conductivity of the sample, the heat is generated in the sample itself (that is to say, if it is more conductive than the material of the tool) or in the tools [9]. Heating rates and pressures applied are quite large, up to 1000 K/min and 150 MPa respectively for graphite tools. This method allows the densification of a whole range of materials such as polymers, metals, ceramics, and composites thereof. A very interesting feature of this process lies in controlling the microstructure generated and its homogeneity in the sample after sintering [10]. The densification rate and the microstructure evolution are controlled by the process parameters such as temperature distribution and pressure throughout the SPS column [1,7].

In the present paper, sintering conditions have been optimized to obtain fully dense TiAl samples, free of carbides, with controlled microstructures (duplex or lamellar), and their creep behaviors were studied.

2. Experimental

2.1. TiAl densification study

Ti-48Al-2Cr-2Nb (TiAl 48-2-2) powder (spherical particles ranging from 33 to 140 μm with D50 = 68 μm) was supplied by SAFRAN Tech and used in this study. More characteristics of this powder are detailed elsewhere [11]. Seven different thermomechanical cycles were performed under vacuum. For each sample, 1.8 g of powder was poured into a graphite mold (8 mm in diameter) whose inner wall was initially
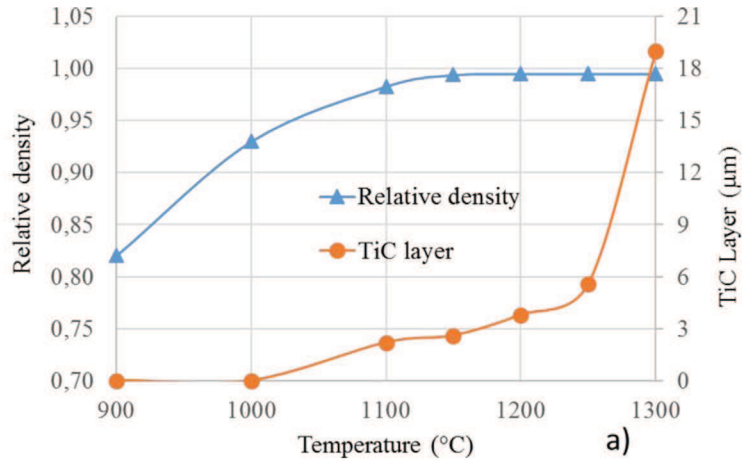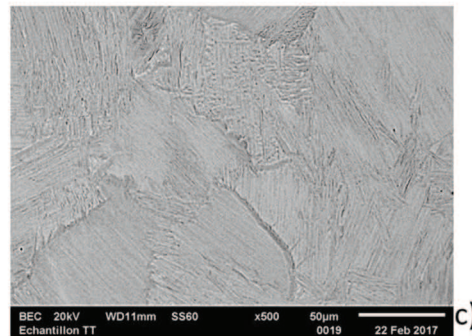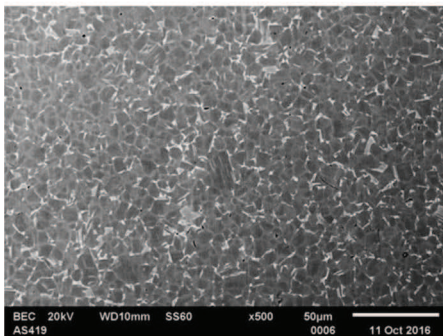
Fig. 1. a) Change in relative density and TiC layer thickness as a function of sintering temperature under 50 MPa; SEM pictures of samples sintered at b) 1200 °C (duplex microstructure) and c) 1300 °C (lamellar microstructure).

covered by graphite foil (Papyex Mersen®). A load of 50 MPa was applied from room temperature to temperatures ranging from 900 to 1300 °C, with a heating rate of 100 °C/min. After reaching maximum temperature, a dwell time of 5 min was applied [12]. For clarity, all temperatures given in the article are the set point programmed at the external surface of the mold; the protocol enabling the determination of the real sintering temperature of samples has been described elsewhere [11]. For this purpose, a specific sintering cycle was performed on a sample, with the temperature monitored by a thermocouple at the surface of the mold and a second one inserted inside the powder bed to measure the sample temperature. Finally, to get the real temperature in the sample, a corrective factor of 1.046 (temperature in °C) should be applied to the temperature measured on the mold surface. At the end of the dwell, the device is switched off, leading to natural cooling of the samples.

The densities of all samples were characterized geometrically. For relative densities greater than 0.95, an extra measurement using the Archimedes method was used to refine results. Fig. 1a summarizes the results obtained for each sample.

The microstructures of all the samples, at the core and next to contact surfaces with graphite molds, were observed using Scanning Electron Microscopy (SEM). One of the main drawbacks of SPS when using such molds and/or graphite foils is that they can react at high temperature with the material to be sintered to form carbides [12]. X-ray diffraction (not shown here) and SEM revealed the presence of a titanium carbide layer at the surface of some TiAl samples. No aluminum carbides were evidenced in the reacted zone, Al probably reacts with the Ti_3Al to form TiAl. The change in thickness of this TiC layer is reported in Fig. 1a as a function of sintering temperature.

For a constant pressure of 50 MPa, full density is reached for temperatures greater than 1150 °C. As for the TiC layer, the reaction seems not sufficiently activated below 1000 °C, and nothing significant was detected. Between 1100 °C and 1250 °C, this layer is between 2 and 6 μm, which is to be compared with the 19 μm-thick layer obtained above 1300 °C.

The growth of such a reaction layer has already been studied by Sudo et al. [13], and more recently by Hayashi et al. [14], on pure titanium samples sintered using SPS under 10 MPa pressure and 5 min to 1 h dwell times at temperatures ranging between 770 and 970 °C. According to these studies, and considering that TiC reaction layer thickness is controlled by diffusion phenomena, results obtained on TiAl were post-processed using the well-established diffusion-rate-controlled parabolic equation $x^2 = kt$. t is the dwell time at maximum temperature, and x represents the thickness of the TiC layer. k is a temperature-activated term given by an Arrhenius equation, $k = k_0 \exp(-Q/RT)$, where Q is the activation energy needed to grow the TiC layer.

From our measurements, an average activation energy of 232.52 kJ/mol was determined. This result is close to the Hayashi et al. [14] estimation of 218.6 kJ/mol for TiC layers grown on pure titanium. Consistently, Khina et al. [15] evaluated the value of the activation energy for TiC layers grown on Ti_3Al samples immersed in carbon powder at between 240 and 460 kJ/mol. All these results are consistent with actual values obtained in this study, and seem to indicate that the growth of the TiC layer is driven by carbon diffusion through the TiC layer.

To investigate the impact of dwell time on TiC layer evolution, four samples with the same previous geometry were sintered at 1250 °C (under 50 MPa with a ramp of 100 °C/min) with dwell times of 0, 1, 5 and 15 min, respectively. Full density was reached for all of them. Assuming diffusion-rate-controlled phenomena, the change in the square of the TiC thickness (x) is plotted as a function of the holding time, Fig. 2. In this case, the linear relationship achieved confirms diffusion control of the reaction and is in agreement with the work of Hayashi et al. [14].

In the study of Hayashi et al., the growth rate of the TiC layer increases from 0.05 μm/min at 770 °C to 0.13 μm/min at 970 °C. In this study, at 1250 °C, the rate rises to 0.38 μm/min.

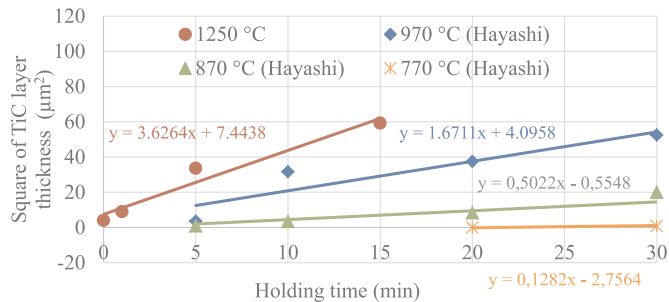Finally, different microstructures were observed after sintering for

Fig. 2. Relationship between square of thickness of TiC coating layer and holding time (results from Hayashi et al. [14]; this study done at 1250 °C).

the different dwell temperatures. In TiAl 48-2-2, the initial duplex microstructure is transformed into a lamellar structure when temperature is above the α transus [16–18]. Voisin et al. [19] confirmed on SPS-sintered 48-2-2 alloy that the duplex-to-lamellar transition temperature is 1335 °C. Consistently, in this study, treatment performed at a dwell temperature of 1300 °C (which in fact, due to temperature gradient in the mold, corresponds to 1360 °C for the powder) are fully lamellar, Fig. 1-c. Below, at 1200 °C, the microstructure remains duplex, Fig. 1-b.

Of course, such differences in microstructure will have an impact on mechanical properties, especially when looking at creep resistance.

2.2. Creep behavior

Metallic alloys generally obey a viscoplastic power law when deformed at high temperatures: $\dot{\varepsilon} = A(T)\overline{\sigma}^n$ (where $\dot{\varepsilon}$ is the generalized strain rate, n a constant coefficient, $\overline{\sigma}$ the von Mises equivalent stress, and $A(T) = A_o exp(-Q/RT)$ where A_o is a constant, Q the activation energy, R the universal gas constant, and T the absolute temperature in K). In a previous study [11], creep parameters in compression were determined at 975 °C according to a revised methodology initially proposed by Manière et al. [20]. For all creep tests, samples were finely polished beforehand to eliminate the carbide layer, which might otherwise have altered the measurements. This characterization was done on duplex microstructures, and coefficients for the Norton law were determined as: $A_0 = 3.14 \, 10^8 \, \text{MPa s}^{-1}$, $Q = 414,163 \, \text{J/mol}$, and $n = 2.81$. The same identification was performed at the same temperature, but this time on fully lamellar microstructure (sample sintered at 1300 °C with a heating rate of 100 °C/min without any dwell under 50 MPa). Fig. 3 summarizes in situ SPS creep tests performed at 975 °C on both microstructures.

After linear regression, creep parameters for a lamellar structure were determined as $A_0 = 32.05 \, 10^3 \, \text{MPa s}^{-1}$, $Q = 384,591 \, \text{J/mol}^{-1}$, and $n = 3.38$. Even though the presence of residual porosities ($\ll 1\%$),
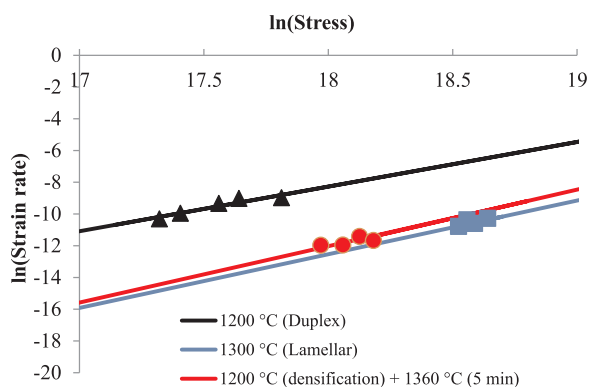

Fig. 3. Change in $\ln(\dot{\varepsilon})$ as a function of $\ln(\sigma)$ at 975 °C for a duplex sample (black), a lamellar sample (blue) and a duplex sample with a heating treatment at 1360 °C (red). (For interpretation of the references to color in this figure legend, the reader is referred to the web version of this article).

these values are in good agreement with those reported by Es-Souni et al. [21] and Tang et al. [22]. According to this result, the stress loading needed to reach equivalent creep rate is four times greater for lamellar structures than for duplex. This improved resistance to creep for lamellar structures relative to duplex structures is well known in the case of TiAl alloys and has been stressed on SPS-densified alloys by Couret et al. [16]. For compression creep tests done at 700 °C under 300 MPa loading, the reported minimum creep rate for lamellar microstructures was $1.10^{-8} \, \text{s}^{-1}$, while for - duplex microstructures, this rate increased to $1.10^{-7} \, \text{s}^{-1}$.

2.3. Annealing treatment to tailor the microstructure

The presence of a TiC layer on TiAl parts can be detrimental given the low ductility of such material at room temperature and the difficulties that can be encountered when machining it, particularly if complex shapes are desired. Such a carbide layer was present in all the samples sintered at high temperature to obtain the lamellar microstructure. A special protocol comprising two separate steps was developed to obtain fully dense lamellar TiAl samples while minimizing the formation of TiC. First, a sample 8 mm in diameter and 10 mm in height was sintered at 1200 °C under 50 MPa. As demonstrated before, this sintering condition leads to full densification and limited TiC layer growth ($< 1 \, \mu\text{m}$). Secondly, the sample was introduced into a graphite mold large enough to avoid any mutual contact (36 mm inner diameter). With this configuration, it was verified that the temperature at the surface of the mold and that of the sample were similar. An annealing treatment at 1360 °C for 5 min was then performed with minimal load applied to the mold to ensure current conduction. The absence of confined contact between the sample and the mold has proven efficient in avoiding TiC layer formation.

Once again, following the methodology described previously, creep parameters were identified: $A_0 = 1.02 \, 10^6 \, \text{MPa s}^{-1}$, $Q = 425,797 \, \text{J/mol}$ and $n = 3.61$. This value for the parameter n is very close to the previous one, indicating similar creep behaviors in both experiments. The short annealing at 1360 °C was sufficient to transform the duplex microstructure of the sample into a lamellar one (SEM micrographs not shown here) without any TiC growth at its periphery.

This two-step method is very interesting, as it allows the production of near-net shape SPS parts made of lamellar TiAl microstructures without machining of the TiC reaction layer.

3. Conclusions

A commercial TiAl 48-2-2 powder was densified by SPS. By optimizing the thermo-mechanical sintering cycle, the dense state is reached for temperatures as low as 1200 °C under 50 MPa. Beyond this temperature, a titanium carbide layer was measured at the surface of the sample. The growth of this layer seems controlled by diffusion rate limited phenomena, like diffusion of carbon in the TiAl matrix or within the TiC layer (Q = 232.52 kJ/mol). Compression creep parameters for duplex and lamellar microstructures were determined, with reduced creep strain rate for the latter, but the presence of the TiC layer is not negligible. An experiment was designed to avoid such TiC layer growth by using a combined densification and annealing SPS cycle.

Prime novelty statement

The dense state is obtained during a densification of a commercial

powder of TiAl 48-2-2 by SPS under a load of 50 MPa at a temperature greater than or equal to 1200 ˚C generating a duplex microstructure.

By densifying this powder at 1300 ˚C by SPS, the microstructure becomes fully lamellar which after mechanical characterization exhibits a better resistance to creep in compression.

At the periphery of the sample, it appears that for a densification at 1200 ˚C, the TiC layer is negligible, contrary to that observed during a thermomechanical cycle at 1300 ˚C. The challenge presented in this paper is to set up an experimental protocol aimed at obtaining a lamellar microstructure without the formation of TiC.

This original approach allows the production of near-net shape SPS parts made of lamellar TiAl microstructures without machining of the TiC reaction layer

References

[1] T. Voisin, Exploration de la voie SPS pour la fabrication d'aubes de turbines pour l'aéronautique: developpement d'un alliage performant et densification de préformes (Ph.D. thesis), Université Toulouse 3 Paul Sabatier (UT3 Paul Sabatier), Toulouse, 2014.
[2] C. Leyens, M. Peters, Wiley VCH, 2003.
[3] D. Hu, X. Wu, M. Loretto, Intermetallics 13 (2005) 914–919.
[4] X. Wu, Intermetallics 14 (2006) 1114–1122.
[5] E. Loria, Intermetallics 9 (2001) 997–1001.
[6] D. Jarvis, D. Voss, Mater. Sci. Eng. 413 (2005) 583–591.
[7] C. Maniere, Spark Plasma Sintering: couplage entre les approches Modélisation, Instrumentation, et Matériaux (Ph.D. thesis), Université T3 Paul Sabatier, 2015.
[8] C. Manière, L. Durand, C. Estournès, Scr. Mater. 116 (2016) 139–142.
[9] Z. Munir, U. Anselmi-Tamburini, M. Ohyanagi, J. Mater. Sci. 41 (2006) 767–777.
[10] R. Orrù, R. Licheri, A. Locci, A. Cincotti, G. Cao, Mater. Sci. Eng. 63 (2009) 127–287.
[11] D. Martins, F. Grumbach, C. Manière, P. Sallot, K. Mocellin, M. Bellet, C. Estournès, Intermetallics 86 (2017) 147–155.
[12] A. Simoulin, Etude du comportement au frittage SPS et au fluage d'un alliage biphasé à base TiAl, internal report -CIRIMAT, 2015.
[13] H. Sudo, I. Tamura, T. Nishizawa, The Microstructure of Metals, Maruzen - Tokyo, 1972, pp. 16.
[14] T. Hayashi, K. Matsuura, M. Ohno, Mater. Transcr. 54 (2013) 2098–2101.
[15] B. Khina, B. Formanck, Physica B 355 (2005) 14–31.
[16] A. Couret, G. Molenat, J. Galy, M. Thomas, Intermetallics 16 (2008) 1134–1135.
[17] J. Murray, Phase Diagrams of Binary Titanium Alloys, ASM International, 1987.
[18] C. McCullough, J. Valencia, C. Levi, R. Mehrabian, Acta Metall. 37 (1989) 1321–1336.
[19] T. Voisin, L. Durand, N. Karnatak, S. Le Gallet, M. Thomas, Y. Le Berree, J. Castagné, A. Couret, J. Mater. Process. Technol. 213 (2013) 269–278.
[20] C. Manière, U. Kus, L. Durand, R. Mainguy, J. Huez, D. Delagnes, C. Estournès, Adv. Eng. Mater. 18 (2016) 1720–1727.
[21] M. Es-Souni, A. Bartels, R. Wagner, Acta Metall. Mater. 43 (1995) 153–161.
[22] J. Tang, B. Huang, Y. He, W. Liu, K. Zhou, A. Wu, Mater. Res. Bull. 37 (2002) 1315–1321.